

# Deuterium Chemical Shift Imaging for the Estimation of Cerebral Perfusion in Rabbit Infarction Model

Kouichi KITO, Toshiyuki ARAI, Kenjiro MORI,  
Shigehiro MORIKAWA\* and Toshiro INUBUSHI\*

In order to develop a new technique for the measurement of local cerebral blood flow (CBF), the deuterium chemical shift imaging ( $^2\text{H}$ -CSI) technique, an application of *in vivo* nuclear magnetic resonance (NMR), was used for the estimation of cerebral perfusion in rabbit infarction model. The  $^2\text{H}$  chemical shift images of rabbit brain were obtained every 30 seconds before and after intravenous injection of deuterated saline. The changes in  $^2\text{H}$  NMR signal intensity documented that the cerebral perfusion in the damaged area due to infarction decreased obviously compared to that in the intact area. These findings indicate that the  $^2\text{H}$ -CSI technique can be applied to the measurement of local CBF. The readily availability and limited toxicity of deuterated water may make possible to use this method in clinical cases. (Key words: cerebral perfusion, deuterium chemical shift imaging, infarction model)

(Kito K, Arai T, Mori K, et al.: Deuterium chemical shift imaging for the estimation of cerebral perfusion in rabbit infarction model. *J Anesth* 7: 447-453, 1993)

Recently developed *in vivo* nuclear magnetic resonance (NMR) techniques are advantageous for the measurement of tissue blood flow in that stable isotope can be used, multiple determinations can be made on the same sample, and imaging experiments can be carried out to determine regional localization. As for the measurement of local CBF, a various NMR imag-

ing techniques using a freely diffusible tracer such as deuterated water ( $\text{D}_2\text{O}$ ), oxygen-17 water ( $\text{H}_2^{17}\text{O}$ ) and gaseous fluorinated compound (FC-23) are reported<sup>1-4</sup>. The technique using a contrast media (Gd-DTPA), which is clinically used for magnetic resonance imaging (MRI), and moreover, the technique not using any tracers are also reported<sup>5,6</sup>. However, there are no reports concerning the application of the deuterium chemical shift imaging ( $^2\text{H}$ -CSI) techniques for this aim.

In this study, to evaluate the feasibility of the  $^2\text{H}$ -CSI for the measurement of local CBF, cerebral perfusion in rabbit infarction model was examined using injected  $\text{D}_2\text{O}$  and  $^2\text{H}$ -CSI.

---

Department of Anesthesia, Kyoto University Hospital, Kyoto, Japan

\*Molecular Neurobiology Research Center, Shiga University of Medical Science, Shiga, Japan

Address reprint requests to Dr. Arai: Department of Anesthesia, Kyoto University Hospital, 54 Kawahara-cho, Shogoin, Sakyo-ku, Kyoto, 606 Japan

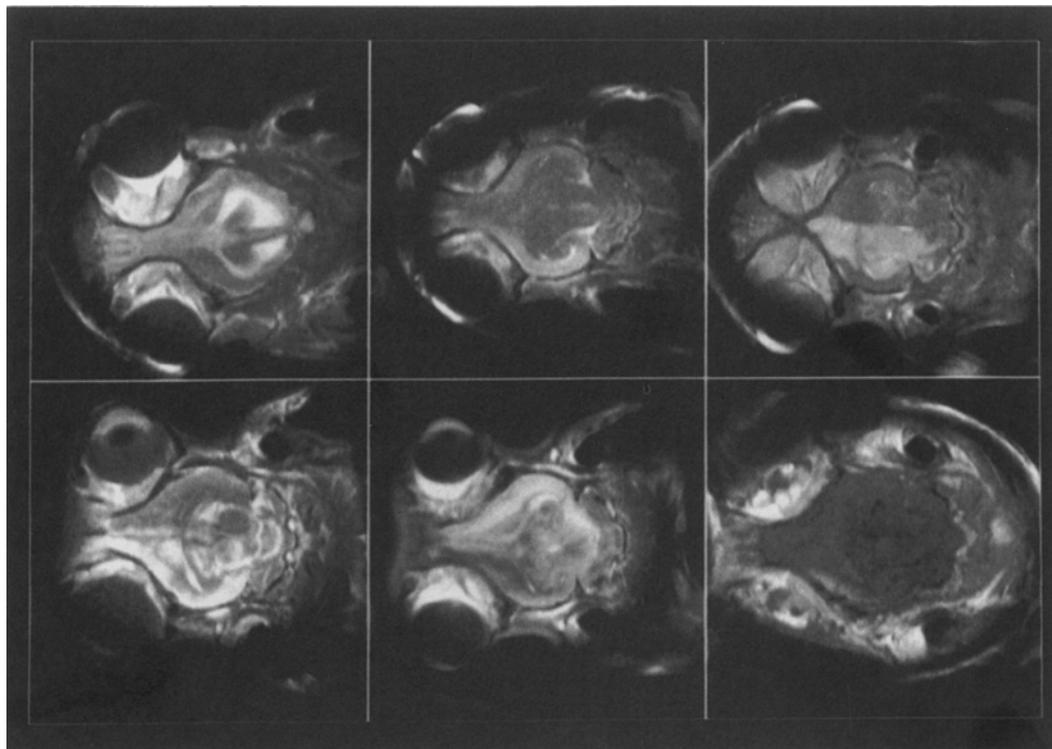


Fig. 1. The axial NMR images of brain obtained from 6 rabbits with infarction. The infarct area is enhanced by Gd-DTPA in each image.

### Materials and Methods

The study protocol was approved by the Animal Investigation Committee of Shiga University of Medical Science. Male New Zealand white rabbits weighing 2–3 kg were used. The animal was anesthetized with 1–2% halothane in 30% oxygen and 70% nitrous oxide, tracheotomized, paralyzed with pancuronium ( $0.5 \text{ mg}\cdot\text{kg}^{-1}$ ), and mechanically ventilated with an animal respirator (model 665, Harvard Apparatus, South Natick, MA). The end-tidal  $\text{CO}_2$  concentration (et  $\text{CO}_2$ ) was monitored continuously by an  $\text{O}_2$ - $\text{CO}_2$  analyzer (Respina, Sanei Co., Tokyo, Japan) and kept between 4.4–5.5%.

The infarction model in rabbit was made using the analogous method reported by Miyazawa et al. in rat<sup>7</sup>. Briefly, the external carotid artery was

cannulated retrograde with polyethylene tube (SP55, Natsume Ltd., Tokyo, Japan) to infuse material into the internal carotid artery. Arterial blood was mixed with an equivolume of ionic contrast media (Meglumine diatrizoate) in a syringe to produce the deformation of red blood cells. Ten ml of the mixed material was infused into the carotid artery for 1 min, which immediately induced the cerebral infarction in the ipsilateral hemisphere.

After these procedures, the animal was positioned prone on a cradle in the bore of the magnet. All NMR images were obtained on a General Electric 2.0 tesla CSI Omega NMR spectrometer/imager equipped with an actively shielded gradient coils which is necessary to perform the chemical shift imaging. A two-turn copper surface coil (7.5 cm in diameter) tuned to both

the proton ( $^1\text{H}$ , 85.6 MHz) and the deuteron ( $^2\text{H}$ , 13.1 MHz) frequency was placed over the head of the animal at the level of eyes.

Before the acquisition of  $^2\text{H}$ -CSI data, the conventional spin-echo  $^1\text{H}$  images were obtained before and after intravenous  $0.5 \text{ mmol}\cdot\text{kg}^{-1}$  of Gd-DTPA injection for the enhancement of the damaged area in the brain. A total of 6 rabbits in which enhanced area by Gd-DTPA was observed on their  $T_1$ -weighted proton NMR image (fig. 1) was used for the following experiments.

The acquisition of  $^2\text{H}$ -CSI data for the estimation of cerebral perfusion was performed with a chemical shift imaging sequence<sup>8,9</sup>. The brain images of an axial section consisting of a  $32 \times 32$  matrix in the 60 mm field of view with a 10-mm slice thickness ( $1.9 \times 1.9 \times 10$  mm in a voxel size) were obtained at 30-second intervals before and after intravenous injection of a 10 ml of 99.8%  $\text{D}_2\text{O}$  in saline. The phase encoding time, repetition time and number of averages were adjusted to get optimum signal-to-noise ratios per unit time.

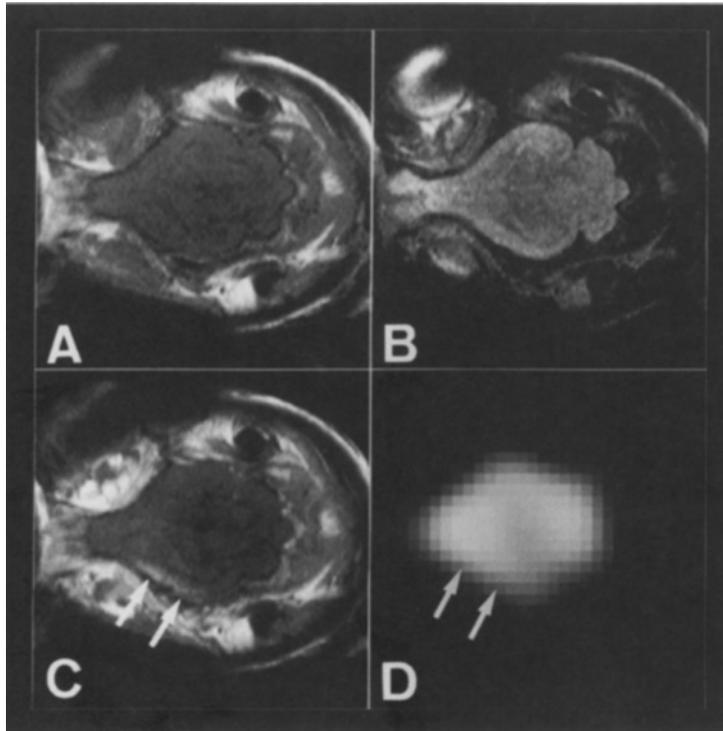


**Fig. 2.** The proton NMR images and chemical shift image.

A) The  $T_1$ -weighted proton NMR image ( $\text{TR}/\text{TE}=500/20$ ) with a  $256 \times 256$  matrix in the 60 mm field of view.

B) The  $T_2$ -weighted proton NMR image ( $\text{TR}/\text{TE}=2000/80$ ).

C) The  $T_1$ -weighted proton NMR image after the injection of Gd-DTPA. The white arrows show the enhanced area by Gd-DTPA.

D) The  $^2\text{H}$  chemical shift image ( $32 \times 32$ ) obtained after the injection of deuterated saline. The white arrows show the hypoperfusion area.

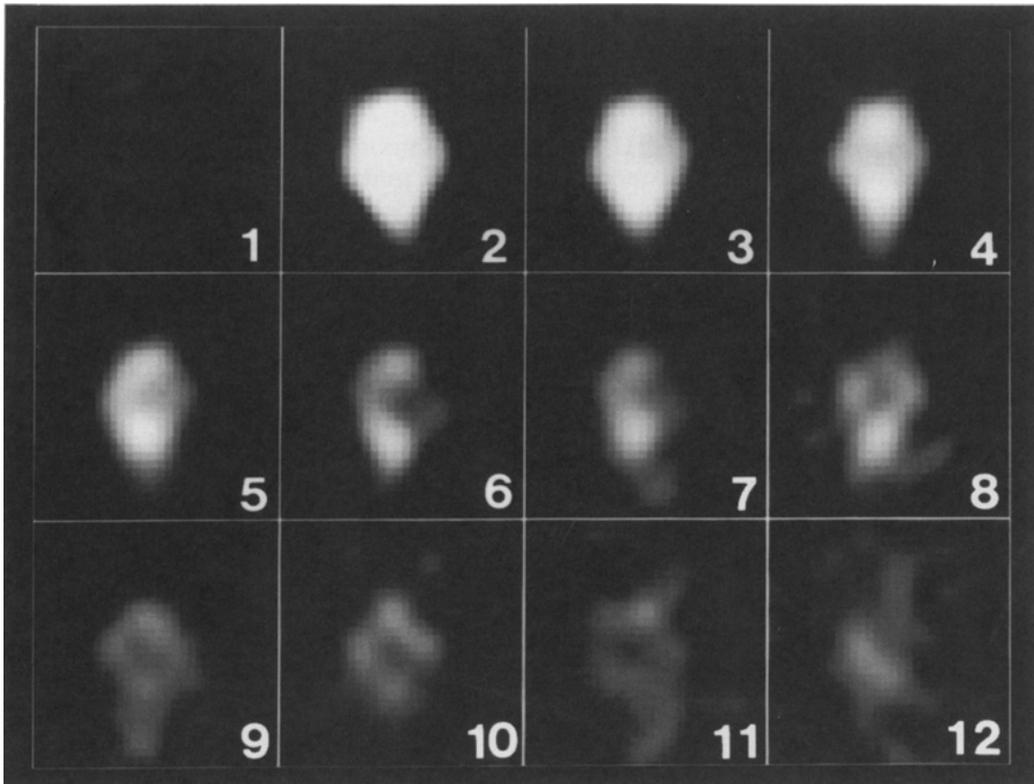


**Fig. 3.** The series of  $^2\text{H}$  chemical shift images, spaced 30 seconds apart, before and after the injection of deuterated saline. The left top corner (No. 1) shows the image before, and others show the images after the injection sequentially (No. 2–12).

As shown in figure 1, the infarct area in each rabbit brain was various in its site, size and extent. Therefore, representative data were shown in the following results.

### Results

Figure 2A and 2B show the conventional  $T_1$ - and  $T_2$ -weighted spin-echo  $^1\text{H}$  brain images in one rabbit, respectively, before the administration of Gd-DTPA. Neither images showed the ischemic changes in brain. However, the  $T_1$ -weighted  $^1\text{H}$  image after the Gd-DTPA injection (fig. 2C) showed the high density area in the hemisphere where the mixture of blood and an ionic contrast media was infused into the carotid artery. Figure 2D shows the  $^2\text{H}$  chemical shift image obtained

at 30 seconds after the  $\text{D}_2\text{O}$  injection. The low density area was observed in the damaged side of the brain.

Figure 3 shows a series of twelve  $^2\text{H}$  chemical shift images obtained at 30-second intervals before and after the injection of  $\text{D}_2\text{O}$ . The changes in the  $^2\text{H}$  NMR signal intensity were shown as those in the image brightness. Although the brain was invisible before the  $\text{D}_2\text{O}$  injection (No. 1), it became visible as soon as  $\text{D}_2\text{O}$  was injected (No. 2) and became less visible gradually (No. 3–12) according to the wash-out of  $\text{D}_2\text{O}$  from the brain. On these images, the low density area in the damaged side of the brain was clearly observed in the images acquired at between 30 to 180 seconds after the  $\text{D}_2\text{O}$  injection (No. 2–7), which became

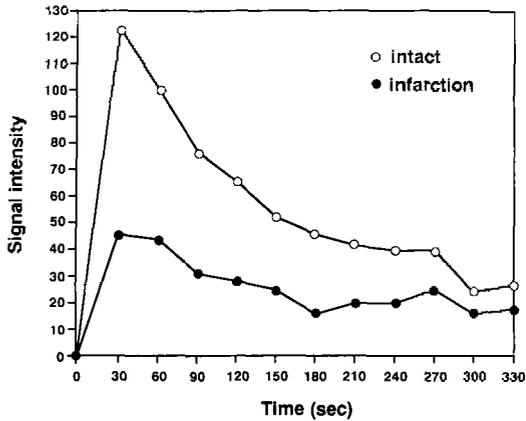


Fig. 4. The changes in  $^2\text{H}$  NMR signal intensity after the injection of deuterated saline. The X axis shows the time in second after the injection. The Y axis shows the signal intensity with an arbitrary unit. The open circles show the signal intensity of intact area, while the closed circles shows that of damaged area.

obscure in the images after that time (No. 8–12).

Figure 4 shows the time-signal intensity curve both in the intact side and in the damaged side, which was measured on figure 3. The signal intensity is proportional to the delivery of  $\text{D}_2\text{O}$  to tissue by local perfusion. By the injection of  $\text{D}_2\text{O}$ , a rapid and acute increase followed by gradual decreases in signal intensity were observed in the intact side of the brain, while a rapid but obtuse increase in signal intensity followed by dull decreases were observed in the damaged side of the brain. At each time after the  $\text{D}_2\text{O}$  injection, the signal intensity in the intact side was higher than that of the damaged side.

### Discussion

Although various NMR imaging techniques to measure local CBF are reported<sup>1–4</sup>, each technique has some drawbacks. For example, the fluorine ( $^{19}\text{F}$ ) NMR imaging technique needs the use of gaseous fluorinated compound (FC-23) as a freely diffusible

tracer<sup>2</sup>. However, since the FC-23 is known to be cardio-toxic<sup>10</sup>, it is not suitable for clinical uses. The techniques using  $\text{H}_2^{17}\text{O}$  as a tracer<sup>3,4</sup> are attractive, because the tracer is non-toxic and may be available in clinical case just like  $\text{H}_2^{15}\text{O}$  used in PET<sup>11,12</sup>. In fact, we also showed the usefulness of  $\text{H}_2^{17}\text{O}$  and  $^{17}\text{O}_2$  with *in vivo*  $^{17}\text{O}$  NMR for the measurement of cerebral blood flow and oxygen consumption<sup>13,14</sup>. However, the terribly high cost of an artificial source disturbs the routine use of oxygen-17 compounds even in small animal experiments. The technique using a contrast media (Gd-DTPA) for MRI as a tracer<sup>5</sup> is suitable for clinical uses, because Gd-DTPA has been already used in clinical cases. However, the method using Gd-DTPA exactly measures not CBF but cerebral blood volume (CBV), because Gd-DTPA cannot diffuse through the blood brain barrier (BBB)<sup>15</sup>. From the point of view of harmlessness, the method to measure local CBF without any tracers<sup>6</sup> is ideal, but the NMR technology for this method is still in progress. On the other hand,  $\text{D}_2\text{O}$  is relatively nontoxic except at very high chronic levels<sup>16</sup>, and  $\text{D}_2\text{O}$  dilution techniques have been already used for measurement of body water in infant, pregnant women and obese subjects in clinical studies<sup>17</sup>.

The imaging experiments of cerebral perfusion using  $\text{D}_2\text{O}$  and  $^2\text{H}$  NMR have been already reported by other investigators<sup>18–20</sup>. However, in their reports, it takes more than 10 minutes to obtain the brain image after  $\text{D}_2\text{O}$  injection, and time resolution is insufficient to follow the changes in brain  $\text{D}_2\text{O}$  concentration for the measurement of CBF. The reason why such a long acquisition time was needed for the  $^2\text{H}$  NMR image formation is that they used the conventional NMR imaging techniques based on the spin-echo or gradient-echo sequence.

In these sequences, the signals of the excited nucleus (those of the  $^1\text{H}$  nucleus are usually specified) are collected after phase encoding steps and during frequency encoding steps under the magnetic gradient<sup>21,22</sup>. These techniques give an excellent spacial resolution in the case of the  $^1\text{H}$  NMR imaging as shown in figure 1. However, in the case of the  $^2\text{H}$  NMR imaging, the  $^2\text{H}$  NMR signals are almost lost during the above-mentioned steps because the  $^2\text{H}$  nucleus has much shorter relaxation times than the  $^1\text{H}$  nucleus. To compensate this loss of the  $^2\text{H}$  NMR signals with signal averaging, a long acquisition time for the  $^2\text{H}$  NMR image formation was needed. In our study, a chemical shift imaging sequence was employed to minimize the loss of the  $^2\text{H}$  NMR signals, because this sequence can skip the frequency encoding steps under the magnetic gradient. As a result, the  $^2\text{H}$  chemical shift image could be obtained every 30 seconds after the injection of  $\text{D}_2\text{O}$  (fig. 3).

Recently, Detre et al. succeeded in the measurement of local CBF with the conventional  $^2\text{H}$  NMR imaging technique<sup>1</sup>. They obtained a series of cat brain images after  $\text{D}_2\text{O}$  injection every 16 seconds, and time resolution was shorter than that in our study. However, unlike our experiments, they injected  $\text{D}_2\text{O}$  via carotid artery. In the case of intracarotid injection, immediate and large increases in brain  $\text{D}_2\text{O}$  concentration occur, which made it possible to measure local CBF with the conventional  $^2\text{H}$  NMR imaging technique. Although the intracarotid injection method is beneficial in animal experiments to measure local CBF, it should be avoided in clinical cases.

The time resolution of 30 seconds is sufficient to follow the changes in brain  $\text{D}_2\text{O}$  concentration for the measurement of CBF in our intravenous injection method. As a matter of fact,

in the CBF measurement by PET, the brain images are collected every 30–60 seconds after the intravenous injection of  $\text{H}_2^{15}\text{O}$ <sup>11,12</sup>. Moreover, the spacial resolution of  $1.9 \times 1.9 \times 10$  mm in a voxel size is also sufficient to localize the  $\text{D}_2\text{O}$  distribution in brain. However, in our study, the quantification of local CBF could not be achieved, because the changes in arterial  $\text{D}_2\text{O}$  concentration were not measured. In the intravenous injection method, the changes in arterial concentration of the tracer as an input function is essential for the CBF calculation<sup>23</sup>. Although the measurement of arterial  $\text{D}_2\text{O}$  concentration can be performed using sampled arterial blood and a high-resolution NMR spectrometer<sup>24</sup>, we omitted those procedures in this preliminary study. However, at least, the distribution of  $\text{D}_2\text{O}$  in brain and its time course could be detected successfully in rabbit infarction model.

In conclusion, the cerebral perfusion in rabbit infarction model could be estimated using intravenously injected  $\text{D}_2\text{O}$  and  $^2\text{H}$ -CSI. The perfusion in the damaged side of brain decreased compared to that in the intact side as expected. Although further studies will be required for the quantification of local CBF, this readily available inert nonradioactive isotope of limited toxicity may provide advantages or alternate routes to measure local CBF in clinical cases.

(Received Oct. 12, 1992, accepted for publication Feb. 16, 1993)

### References

1. Detre JA, Subramanian VH, Mitchell MD, et al: Measurement of regional cerebral blood flow in cat brain using intracarotid  $^2\text{H}_2\text{O}$  and  $^2\text{H}$  NMR imaging. *Magn Reson Med* 14:389–395, 1990
2. Branch CA, Helpert JA, Ewing JR, et al:  $^{19}\text{F}$  NMR imaging of cerebral blood flow. *Magn Reson Med* 20:151–157, 1991

3. Pekar J, Ligeti L, Ruttner Z, et al: In vivo measurement of cerebral oxygen consumption and blood flow using  $^{17}\text{O}$  magnetic resonance imaging. *Magn Reson Med* 21:313-319, 1991
4. Kwong KK, Hopkins AL, Belliveau JW, et al: Proton NMR imaging of cerebral blood flow using  $\text{H}_2^{17}\text{O}$ . *Magn Reson Med* 22:154-158, 1991
5. Rudin M, Sauter A: Noninvasive determination of regional cerebral blood flow in rats using dynamic imaging with Gd(DTPA). *Magn Reson Med* 22:32-46, 1991
6. Detre JA, Leigh JS, Williams DS, et al: Perfusion imaging. *Magn Reson Med* 23:37-45, 1992
7. Miyazawa T, Nakagawa H, Oshino N: Role of red blood cell deformation in toxicity of contrast media in cerebral angiography. *Invest Radiol* 24:383-389, 1989
8. Brown TR, Kincaid BM, Ugurbil K: NMR chemical shift imaging in three dimensions. *Proc Natl Acad Sci USA* 79:3523-3526, 1982
9. Haselgrove JC, Subramanian VH, Leigh JS Jr, et al: In vivo one-dimensional imaging of phosphorous metabolites by phosphorous-31 nuclear magnetic resonance. *Science* 220:1170-1173, 1983
10. Avidio DM: Toxicity of aerosol propellants in the respiratory and circulatory systems: X. Proposed classification. *Toxicology* 3:321-332, 1975
11. Herscovitch P, Markham J, Raichle ME: Brain blood flow measured with intravenous  $\text{H}_2^{15}\text{O}$ . I. Theory and error analysis. *J Nucl Med* 24:782-789, 1983
12. Raichle ME, Martin WRW, Herscovitch P, et al: Brain blood flow measured with intravenous  $\text{H}_2^{15}\text{O}$ . II. Implementation and validation. *J Nucl Med* 24:790-798, 1983
13. Arai T, Nakao S, Mori K, et al: Cerebral oxygen utilization analyzed by the use of oxygen-17 and its nuclear magnetic resonance. *Biochem Biophys Res Commun* 169:153-158, 1990
14. Arai T, Mori K, Nakao S, et al: In vivo oxygen-17 nuclear magnetic resonance for the estimation of cerebral blood flow and oxygen consumption. *Biochem Biophys Res Commun* 179:954-961, 1991
15. Lassen NA: Cerebral transit of an intravascular tracer may allow measurement of regional blood volume but not regional blood flow. *J Cereb Blood Flow Metab* 4:633-634, 1984
16. Peng S-K, Ho K-J, Taylor CB: Biologic effects of prolonged exposure to deuterium oxide: A behavioral, metabolic, and morphologic study. *Arch Path* 94:81-89, 1972
17. Coward WA: Deuterium method for measuring milk intake in babies. *Lancet* 309, 1979
18. Ewy CS, Babcock EE, Ackerman JJH: Deuterium nuclear magnetic resonance spin-imaging of  $\text{D}_2\text{O}$ : A potential exogenous MRI label. *Magn Reson Imaging* 4:407-411, 1986
19. Muller S, Seelig J: In vivo NMR imaging of deuterium. *J Magn Reson* 72:456-466, 1987
20. Ewy CS, Ackerman JJH, Balaban RS: Deuterium NMR cerebral imaging in situ. *Magn Reson Med* 8:35-44, 1988
21. Kumar A, Welti D, Ernst RR: NMR fourier zeugmatography. *J Magn Reson* 18:69-83, 1975
22. Edelstein WA, Hutchison JMS, Johnson G, et al: Spin warp NMR imaging and applications to human whole-body imaging. *Phys Med Biol* 25:751-756, 1980
23. Zierler KL: Equations for measuring blood flow by external monitoring of radioisotopes. *Circ Res* 16: 309-321, 1965
24. Brereton IM, Irving MG, Field J, et al: Preliminary studies on the potential of *in vivo* deuterium NMR spectroscopy. *Biochem Biophys Res Commun* 137:579-584, 1986